atmosphere

MDPI

*Article*

# Organic Vapors from Residential Biomass Combustion: Emission Characteristics and Conversion to Secondary Organic Aerosols

**Ruijie Li [1], Siyuan Li [2,*], Xiaotong Jiang [3], Yangzhou Wu [4] and Kang Hu [5]**

[1] Beijing Weather Modification Center, Beijing Key Laboratory of Cloud, Precipitation and Atmospheric Water Resources, Beijing Meteorological Service, Beijing 100089, China; leeruijie0905@sina.com
[2] Department of Atmospheric Sciences, School of Earth Sciences, Zhejiang University, Hangzhou 310030, China
[3] College of Biological and Environmental Engineering, Shandong University of Aeronautics, Binzhou 256600, China; xtjiang@zju.edu.cn
[4] Guangxi Key Laboratory of Environmental Pollution Control Theory and Technology, College of Environment Science and Engineering, Guilin University of Technology, Guilin 541004, China; wuyangzhou@glut.edu.cn
[5] Jiangsu Collaborative Innovation Center of Atmospheric Environment and Equipment Technology, Jiangsu Key Laboratory of Atmospheric Environment Monitoring and Pollution Control, Nanjing University of Information Science & Technology, 219 Ningliu Road, Nanjing 210044, China; 200060@nuist.edu.cn
* Correspondence: siyuanli@zju.edu.cn

**Abstract:** Residential biomass combustion emits a large amount of organic gases into ambient air, resulting in the formation of secondary organic aerosol (SOA) and various environmental and health impacts. In this study, we investigated the emission characteristics of non-methane organic compounds (NMOCs) from residential biomass fuels during vigorous combustion (flaming) and stable combustion (smoldering) conditions. We quantified NMOC emission factors based on the CO concentration for different combustion phases and found that NMOC emissions were higher during the smoldering phase and approximately two to four times greater than those during flaming. NMOCs were categorized into volatile organic compounds (VOCs) and intermediate-volatility organic compounds (IVOCs) through the modeling of the organic compound volatility distribution. The photochemical aging of NMOCs revealed furans, phenolics, and certain IVOCs as significant non-traditional SOA precursors, with over half being consumed during a short aging period. A parametric function was established, indicating that accounting for non-traditional SOA precursors and IVOC yields improves the representation of the net enhancement of measured organic aerosol (OA). This study emphasizes the importance of differentiating emissions from various phases of residential biomass combustion and recognizing non-traditional SOA precursors and IVOCs for accurate SOA assessment and prediction.

**Keywords:** residential biomass combustion; non-methane organic compounds (NMOCs); emission characteristics; flaming and smoldering; secondary organic aerosol (SOA)

check for updates

**Citation:** Li, R.; Li, S.; Jiang, X.; Wu, Y.; Hu, K. Organic Vapors from Residential Biomass Combustion: Emission Characteristics and Conversion to Secondary Organic Aerosols. *Atmosphere* **2024**, *15*, 692. https://doi.org/10.3390/atmos15060692

Academic Editor: Pilar Fernández Ramón

Received: 18 April 2024
Revised: 22 May 2024
Accepted: 4 June 2024
Published: 6 June 2024

**Copyright:** © 2024 by the authors. Licensee MDPI, Basel, Switzerland. This article is an open access article distributed under the terms and conditions of the Creative Commons Attribution (CC BY) license (https://creativecommons.org/licenses/by/4.0/).

## 1. Introduction

Residential biomass combustion is a significant source of energy globally, producing substantial emissions of organic compounds that adversely affect human health and the climate [1,2]. These emissions include a variety of gaseous organic species, notably non-methane organic compounds (NMOCs), such as volatile organic compounds (VOCs) and intermediate-volatility organic compounds (IVOCs) [3,4]. In recent years, the Chinese government has introduced stringent and effective emission reduction measures and has made significant progress in reducing pollutant emissions from coal combustion [5]. Consequently, residential biomass combustion is now receiving increasing attention from the air quality research community.

The organic gases and particulate matter found in biomass combustion plumes are composed of thousands of distinct compounds, with the complexity of their composition

being influenced by several factors, including operational conditions, combustion technologies, and fuel types [6]. Moreover, varying combustion phases also result in different emission characteristics [7]. The volatility, reactivity, and other properties of these compounds vary greatly [8,9]. The volatility of organic compounds dictates their presence in gas or particulate phases, and it is typically measured as the saturated mass concentration ($C_0$) [10]. Functionalization reactions can decrease volatility, while fragmentation reactions can increase volatility [11,12]. Consequently, these organic substances continuously undergo transformations in the atmospheric environment.

In recent years, most studies have focused on the primary emission characteristics of NMOCs from rural residential biomass combustion, with limited knowledge of the photochemical oxidation of smoke plumes entering the atmosphere after combustion [13–15]. NMOCs can react with atmospheric oxidants, such as hydroxyl radicals (OH·). Through atmospheric chemical oxidation, NMOCs are rapidly oxidized to form low-volatile condensable products and contribute to the formation of secondary organic aerosol (SOA) [16,17]. The particulate matter generated from the oxidation of NMOCs is also an important component of biomass burning emissions. Moreover, compared to VOCs with higher volatility, some IVOCs are more likely to form particulate matter due to their lower $C_0$ under the same atmospheric oxidation conditions. This is an often overlooked yet crucial aspect when assessing the production of organic matter from biomass combustion [18].

The effect of atmospheric secondary aging processes on residential biomass combustion NMOCs is being increasingly recognized. Numerous studies have explored the aging mechanism through laboratory modeling and atmospheric observations. For instance, Niu et al. used an oxidation flow reactor to demonstrate the emission characteristics of fresh and aged VOCs by burning a range of biomass fuels that are commonly used in rural areas [19]. Akherati et al. demonstrated that oxygenated aromatic hydrocarbons undergo rapid oxidation processes near the source, contributing to the generation of SOA. Another study showed that aromatic hydrocarbons and terpenes decreased in concentration during aging, while formic acid and other unidentified oxidation products increased [17]. A recent study reviewed the chemistry and gas-phase products of furanoids from biomass burning, their interactions with major atmospheric oxidants, and the generation of SOA. It provided new insights into the atmospheric behaviors of furans and their impact on air quality [20]. Other studies have quantified gaseous organic compounds from biomass combustion through extensive experiments, identified potential SOA precursors, and assessed the impact of VOCs from biomass combustion on organic aerosol formation [21,22]. However, NMOC emissions from residential biomass combustion vary greatly due to diverse fuel types and combustion conditions, leading to significant uncertainty in atmospheric aging results [23–25]. Therefore, it is necessary to conduct aging experiments that incorporate actual combustion and real atmospheric conditions, providing crucial data for exploring the NMOC reaction mechanism.

Furthermore, some studies have indicated that a significant portion of NMOCs emitted from biomass burning are IVOCs, and their emission characteristics and role in SOA formation are not yet fully understood [26,27]. Research has indicated that besides oxidizing to transform lower volatility compounds into the particulate phase, IVOCs may also directly undergo gas–particle conversion with particulate matter as the ambient saturation vapor pressure changes [28,29]. The interactive processes between NMOCs and particulate matter include the gas-phase oxidation of VOCs, the formation of SOA through gas–particle partitioning, and the oxidation of organic vapors that volatilize from existing particles after plume dilution. However, there is still considerable uncertainty regarding the reactive characteristics of VOCs and IVOCs from residential biomass burning in the atmosphere and their contributions to SOA formation.

In view of this, we focused on commonly used residential fuels, establishing a combustion laboratory to simulate the emissions from residential biomass burning. Additionally, by employing a smog chamber aging system, we simulated the atmospheric photochemical aging process of NMOCs. To investigate different species and proportions of VOCs and

IVOCs, we collected plume under different conditions and analyzed the aging process in detail for VOCs and IVOCs, respectively. The aim of this study was to explore the emission characteristics of organic vapors from biomass burning and their contributions to the formation of SOA.

## 2. Materials and Methods

### *2.1. Combustion and Aging Experiments*

The combustion experiments in this study were carried out in the combustion laboratory at the Beijing Weather Modification Science Experiment Base, located in Pinggu District, northwestern Beijing (40°10′44.16″ N, 117°8′43.59″ E).

A traditional residential combustion stove was used, with sun-dried apple wood serving as the fuel; approximately 200 g was used for each ignition. A block of solid alcohol was employed to ignite the wood, and efforts were made to maintain uniformity in the size of the firewood across experiments. The emissions from the combustion were discharged through a 2-meter-high vertical stainless steel flue. For details on combustion experiments and sampling, see the previous study [30].

To evaluate the impact of various combustion conditions on the NMOCs released from biomass burning and their subsequent atmospheric aging, two distinct ignition approaches were implemented. The first method involved increasing the oxygen supply and rapidly igniting the fuel to form an intense flame with a higher combustion efficiency and fewer flue gas emissions. The second method involved adding an equal mass of fresh fuels at a later stage of combustion of the existing fuel and allowing it to ignite naturally. This slower and less efficient combustion produced more flue gas emissions. The modified combustion efficiency (MCE) values for these two combustion methods were calculated to be approximately 0.95 and 0.80, representing the flaming condition and the smoldering condition, respectively.

Aging experiments for NMOCs were conducted in a polytetrafluoroethylene (PTFE) plume aging chamber, the specifics of which were reported in the previous study by Li et al. [31]. Before the aging experiments, the chamber was flushed with pure air to reduce the particulate concentration to near zero. We performed aging tests on the plume from the flaming condition and the smoldering condition, respectively, with photochemical reactions triggered by natural sunlight outside. Throughout the aging process, filtered ambient air was introduced at a rate of approximately 2 L per minute to simulate atmospheric plume dilution and replenish reacted oxidants. These aging tests lasted approximately 4 h. During this time, the sample plume in the chamber was monitored using advanced real-time monitoring instruments.

### *2.2. Sampling and Analysis*

The gaseous organic compounds were measured using a PTR-ToF-MS (Ionicon Analytik, GmbH Innsbruck 8000, Eduard-Bodem Austria). $H_3O^+$ was selected as the reagent, which is particularly well suited for analyzing samples that contain a variety of trace gases [32]. The average count rate of $H_3O^+$ was $3.3 \times 10^6$ counts $s^{-1}$ (cps). The PTR was operated with a drift tube pressure of 2.2 mbar, a chamber temperature of 60 °C, and a drift voltage of 600 V. The energy density (E/N) was approximately 135 Td (1 Td = $10^{-17}$ V $cm^3$ molecule). VOC-free zero air was generated through a VOC scrubber catalyst heated at 350 °C to measure the background value.

The sampling data were analyzed using the Ionicon Analytik GmbH software (PTR-MS Viewer, version 3.1.0). Mass calibration was performed using $H_3O^+$ ($m/z$ = 21.023), $CH_3COCH_4^+$ ($m/z$ = 59.049), and monoterpenes ($m/z$ = 137.129). Prior to each experiment, offsets against the $m/z$ were calibrated. Calibration was carried out by employing a multi-component gas standard (GCU-advanced 2.0) containing 1 ppm ± 5% of formaldehyde, methanol, acetonitrile, acetaldehyde, acetone, methyl ethyl ketone, isoprene, benzene, toluene, styrene ethylbenzene, and 1,3,5-trimethylbenzene [33]. The complexity of VOC species from biomass combustion does not allow for the calibration of all organic gases

during the experiment. The relative transport efficiencies of $H_3O^+$ and $MH^+$ (M for organic gases) ions through the drift tube and the mass spectrometer can be estimated from the transport efficiency curves. To convert the raw PTR-ToF-MS signal to a concentration, it is essential to determine the reaction rate constant of each species with the reagent in the drift tube. Due to the relatively limited number of measurable reaction rate constants, it is not possible to assign a reaction rate constant for each ion. When available, individual reaction rate constants are applied from the literature [34,35], and a default reaction rate constant of $2.0 \times 10^{-9}$ cm $s^{-1}$ can be applied to all other ions.

Throughout the experiment, the mass of reacted NMOGs was measured, and their contribution to SOA was determined using reported SOA mass yields [36–38]. Non-refractory particulate emissions were measured using a high-resolution time-of-flight aerosol mass spectrometer (AMS, Aerodyne Research, Inc. Billerica, MA, USA). The instrument was employed to monitor the change in actual organic aerosol (OA), with the amount of SOA being calculated as the difference between the total OA after aging and POA.

### *2.3. Parameterizations of NMOC Volatility*

The $C_0$ value is one of the key thermodynamic properties describing the volatility of organic compounds. We predicted $C_0$ as a function of the elemental composition, typically determined by soft-ionization high-resolution mass spectrometry. The model formulation was developed by Donahue and Li et al. as follows [39,40]:

$$log_{10}C_0 = \left(n_C^0 - n_o\right)b_C - n_o b_O - 2\frac{n_c n_o}{n_c + n_o}b_{co} - n_N b_N - n_S b_S \quad (1)$$

where $n_C^0$ is the reference carbon number; $n_c$, $n_o$, $n_N$, and $n_S$ are the numbers of C, O, N, and S atoms, respectively; and $b_C$, $b_O$, $b_N$, and $b_S$ are the contributions of each atom to $log_{10}C_0$, respectively. Values of b coefficients for each class (CO, CH, CHO, CHN, CHON, CHOS, and CHONS) were obtained from a multilinear least-squares fit of 30,000 compounds from the research by Li et al. [40].

## 3. Results and Discussion

### *3.1. NMOC Spectrum of Residential Biomass Combustion Emissions*

Typical PTR-TOF-MS spectra of plumes and ambient air are shown in Figure 1. The complexity of biomass burning (BB) emissions poses a challenge for mass spectral interpretation and emission characterization. PTR-ToF-MS scans possess high resolution, enabling the identification of the molecular formula of a specific ion peak through a precise mass measurement and a comparison with potential candidate molecular formulas for the protonated compound. If only one compound is structurally plausible or has been definitively identified and confirmed in previous BB studies [27,41], this study will recognize the compound-specific identifiers of candidate molecular formulas.

Figure 1a–c depict the NMOC mass spectra of a typical flaming condition and smoldering condition from combustion experiments and ambient atmospheric air. The intensity of the mass spectral signals indicates that NMOCs emitted during the combustion experiments (flaming and smoldering) were notably higher than those in the ambient atmosphere, with NMOCs exhibiting greater abundance in the smoldering phase compared to the flaming phase. This phenomenon may be attributed to the differing combustion conditions and mechanisms between the flaming and smoldering phases. The lower MCE during smoldering, with a lower combustion temperature and reduced oxygen supply, causes most of the fuel to undergo pyrolysis reactions, forming particulate matter or gases. Consequently, most of the organic matter cannot be fully oxidized to $CO_2$, resulting in the formation of various NMOCs [41–43]. Measurements of ambient NMOCs were chosen before the combustion experiment in each experiment or when conducting blank control experiments. NMOCs in the ambient atmosphere are mainly concentrated in the small molecule organic matter category, and there are very few NMOCs with a relative molecular mass greater

than $m/z$ 130 (raw signal less than 0.35). In contrast, biomass combustion produces more NMOCs with larger molecular organic matter. Most of these are IVOCs, which are more likely to produce SOA through oxidation as these are less volatile.

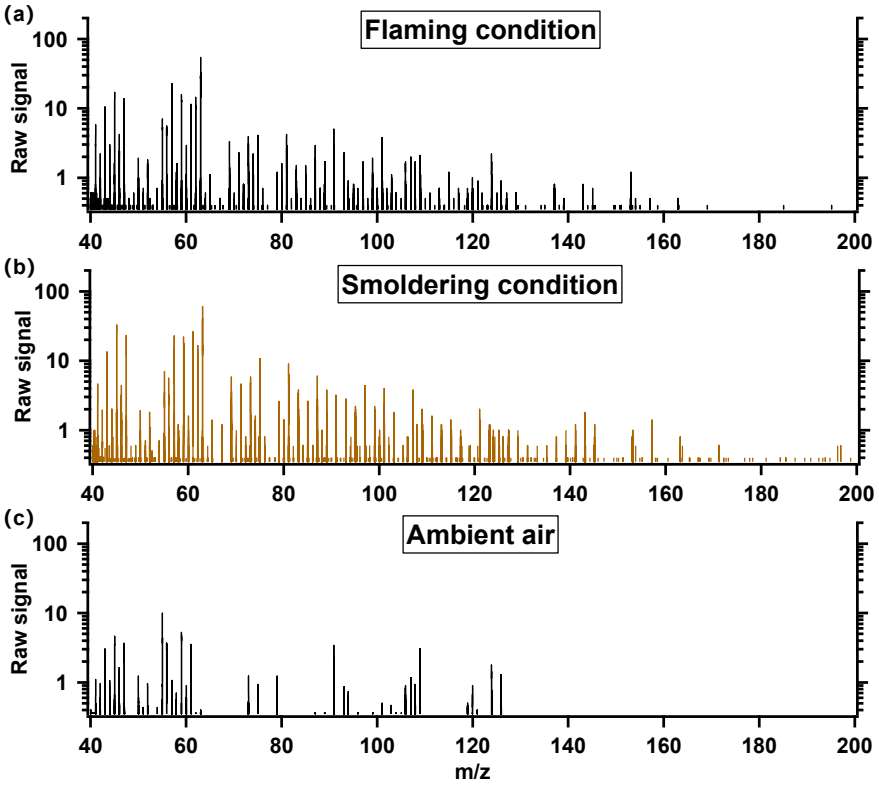



**Figure 1.** Typical mass scan of biomass burning plume from PTR-TOF-MS. (**a**) Initial emission of gas-phase non-methane organic compounds (NMOCs) from flaming burning phase. (**b**) Initial emission of NMOCs from smoldering burning phase and (**c**) observation of real ambient atmospheric NMOCs during experiments.

### *3.2. Emission Characteristics of NMOCs at Different Combustion Conditions*

We classified the measured NMOCs into seven categories based on their functional groups: furans, carboxylic acids, phenols, aromatic hydrocarbons, nitrogen-containing compounds, aliphatic hydrocarbons, and carbonyl compounds. Figure 2 shows the emission factors for each type of NMOC normalized to the concentration of ΔCO. Δ[NMOCs] and Δ[CO] are the excess mixing ratios of NMOCs and CO. To compute the excess quantities, we assume that the background values of NMOCs and $CO_2$ are ambient concentrations. Figure 2 illustrates that the emission characteristics of NMOCs from residential biomass combustion are significantly influenced by combustion conditions. For the same fuel type and weight, all types of NMOCs show higher emission factors during the smoldering phase compared to the flaming phase.

Among these species, carbonyl compounds were the most abundant (mainly aldehydes and ketones compounds), including acetaldehyde ($m/z$ = 45.03), acrolein ($m/z$ = 57.03), acetone ($m/z$ = 59.05), ethanol aldehyde ($m/z$ = 61.03), methylglyoxal ($m/z$ = 73.03), and hydroxyacetone ($m/z$ = 75.04), which accounted for about 26% of all species. In previous biomass combustion studies [26,35], carbonyl compounds have also been shown to dominate as the main components of NMOCs emitted from combustion. These substances are highly reactive, and most of them will participate in chemical reactions in the atmosphere. Notably, carbonyl compounds, as a major source of atmospheric organic acids, promote the formation of SOA [44,45]. In addition, carbonyl compounds can also serve as intermediate oxidation products after the primary reaction of some VOCs with free radicals, which can originate from the secondary formation of photochemicals [46].

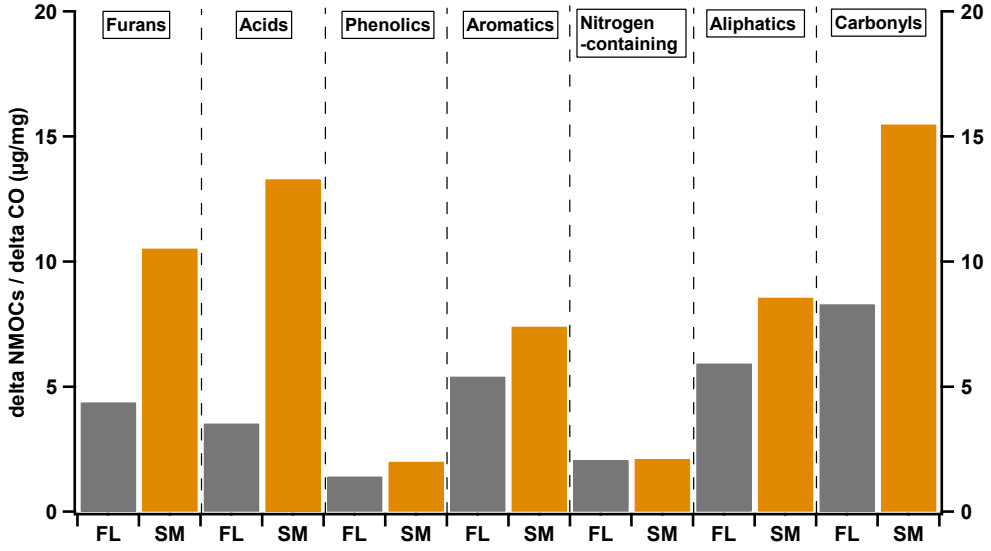



**Figure 2.** Average emission factors of VOCs from combustion for each flaming (FL) and smoldering (SM) experiment. EFs-VOCs based on CO are calculated based on initial concentrations, measured from chamber with PTR-MS.

Aromatic hydrocarbons also constitute a significant fraction of NMOCs emitted from biomass combustion. Benzene ($m/z$ = 79.05) is the predominant aromatic compound, representing 56% and 48% of the total aromatic hydrocarbon emissions during the two distinct combustion phases, respectively. Previous research has indicated that the combustion of domestic biomass and open wildfires are the principal contributors to benzene emissions globally [47,48]. Other notable aromatics include toluene ($m/z$ = 93.07), styrene ($m/z$ = 105.07), xylene/ethylbenzene ($m/z$ = 107.09), and 1,3,5-trimethylbenzene ($m/z$ = 121.10). Naphthalene ($m/z$ = 129.07) and its derivatives, which belong to polycyclic aromatic hydrocarbons (PAHs), exhibit volatility ranging from intermediate volatility to semi-volatile, and they can serve as significant precursors for SOA [34]. The chemical reactions of aromatic hydrocarbons are influenced by various oxidative pathways, with the complexity of these reactions largely being driven by the reactivity of the OH radical [49,50]. The aging of these gas-phase aromatic hydrocarbons in an aging chamber can result in the formation of species with lower volatility and potential condensation into the particulate phase. While aromatic hydrocarbons possess a high potential for SOA formation, their actual efficiency in generating SOA is influenced by several environmental factors, such as relative humidity, temperature, aerosol mass concentration, $NO_x$ levels, and the concentration of $RO_2$ radicals [48,51].

Phenolics are mainly composed of phenol ($m/z$ = 95.05) and cresol ($m/z$ = 109.07), which account for more than 60% of all phenolics. They mainly form during cellulose pyrolysis in biomass combustion. Several studies have indicated that phenolic compounds play a crucial role in SOA formation [26,52]. However, there is a large amount of uncertainty regarding the emission factors for phenolic compounds, which are closely related to the type of fuel and the combustion furnace used.

It is notable that substantial emissions of furans were detected during both flaming and smoldering combustions, constituting a significant proportion of the total NMOC emissions, roughly 10% to 20%. The identified furan compounds included furan ($m/z$ = 69.034), methylfurans ($m/z$ = 83.049), furfural (furan formaldehyde, $m/z$ = 97.028), furan methanol ($m/z$ = 99.044), methylfurfural ($m/z$ = 111.044), benzofurans ($m/z$ = 119.049), hydroxymethylfurfural ($m/z$ = 127.039), and numerous other furan derivatives. Furan compounds are predominantly generated from the pyrolysis of cellulose, with emissions being especially pronounced during the smoldering phase and significantly higher than those of aromatic hydrocarbons. Research indicates that in contrast to phenolic compounds, furans and their derivatives were the predominant species in combustion emissions across various

fuel types [26]. Despite being relatively less studied, furans, as unsaturated heterocyclic compounds in biomass combustion emissions, are acknowledged as key non-traditional SOA precursors, similar to phenolics [53,54]. Note that under atmospheric conditions, acid catalysis can promote the gas-phase cyclization of carbonyl compounds to furans. However, this process may be limited in complex pollutant mixing environments due to factors such as competition with other atmospheric reactions [55]. It has been demonstrated that furans, including 2-methylfuran and 3-methylfuran, along with their reaction intermediates, can undergo photochemical oxidation to contribute to the formation of SOA in smog chamber aging experiments. However, comparatively fewer studies have focused on oxygenated furans, such as furfural. In this work, furans with oxygen-functional groups are the main constituents emitted from combustion. These furans can transform during the photochemical aging process, which is further discussed in Section 3.3.

NMOCs emitted from combustion also include nitrogen-containing species and aliphatic hydrocarbons. In this study, a limited number of distinctive nitrogen-containing peaks were subjected to fitting and analysis. Only a few nitrogen-containing species were observed in quantifiable amounts, with some unable to be definitively associated with a specific chemical formula or definite relative contribution value. The species enumerated in Table S2 are derived from previous biomass burning experiments [26,35,56]. Aliphatic hydrocarbons also experienced some fragmentation interference. For instance, ethylene ($C_2H_4$) and hydrocyanic acid (HCNH) caused signal interference at $m/z$ 28; similarly, propylene and other alkenone fragments interfered at $m/z$ 43. Other alkene and hydrocarbon fragments were also present at $m/z$ 53, 57, and 67. Specifically, the signal at $m/z$ 57 was mainly attributed to acrolein and butene. In the analysis of combustion emissions, the acrolein signal peak is typically more pronounced.

### *3.3. Transformation of NMOCs during Photochemical Aging*

Combustion-emitted NMOCs were exposed to natural sunlight within a smog chamber that mimics real atmospheric conditions, initiating a series of atmospheric oxidation reactions. Acetonitrile, the primary emission from biomass combustion, was utilized to calibrate the wall loss effect of NMOCs in the chamber due to its relatively low atmospheric reactivity. After a 4 h reaction period and the calibration of acetonitrile concentrations, substances exhibiting a marked reduction in concentration, indicating their involvement in the oxidation process, were identified as gaseous precursors of SOA. This study will focus on furans and phenols, which are recognized as non-traditional SOA precursors and have attracted significant interest in recent years.

As depicted in Figure 3, furans and several of their derivatives, such as methylfuran, furfural, C2/C3-substituted furan, 5-methyl furfural, and benzofuran, experienced notable reductions during the atmospheric photochemical reactions, with the concentrations of methylfuran and furfural being decreased by over 50%. Moreover, the observed decline in concentration at which furans decreased was consistently more pronounced in the smoldering aging experiments compared to that in the flaming aging experiments. When exposed to OH radical concentrations ranging from $1.2 \times 10^6$ to $2.3 \times 10^6$ molecules $cm^{-3}$, as shown in Figure 4b, furans underwent significant chemical transformations.

In addition to the simultaneous consumption of furans in both flaming and smoldering aging experiments, certain furan compounds increased, such as nitrofuran and 5-Hydroxymethylfurfural. This observed increase may be partly due to their formation as oxidizing by-products of furans and methylfurans, but they may also be due to the volatilization of OA or the degradation of SOA. Given that the reaction process is dynamic, the VOCs released through volatilization, along with those produced as intermediate oxidation species, are subject to further oxidation. Figure 4c shows the molecular corridors of molar mass vs. the saturation mass concentration of furans; photochemical reactions lead to the generation of certain oxidation intermediates of VOCs and IVOCs. This phenomenon may affect the calculation of furan SOA yields to some extent and exacerbate the challenges associated with assessing the SOA from furans and IVOCs.

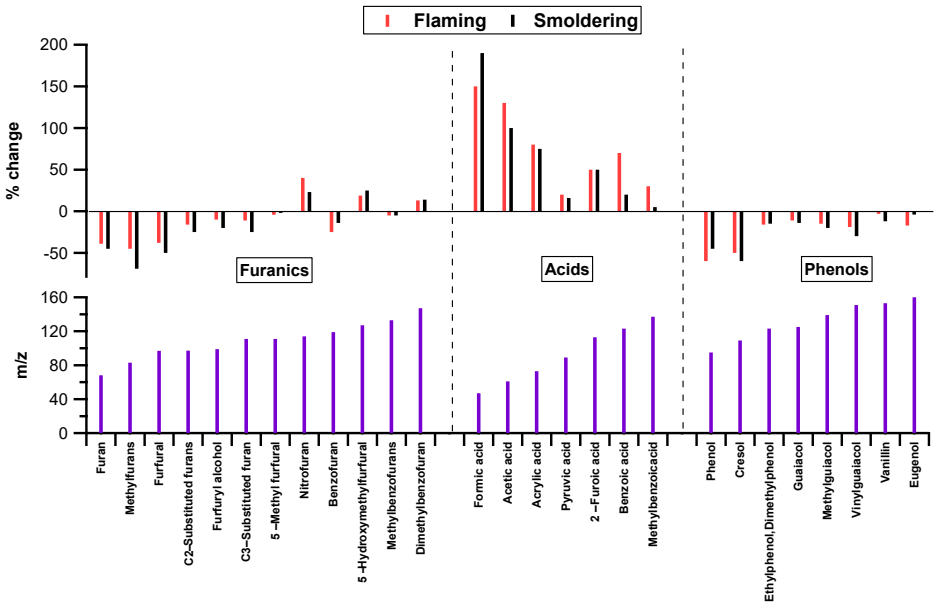



**Figure 3.** Changes in the mass ratio of NMOCs from flaming and smoldering experiments during photochemical aging, relative to the initial concentration.

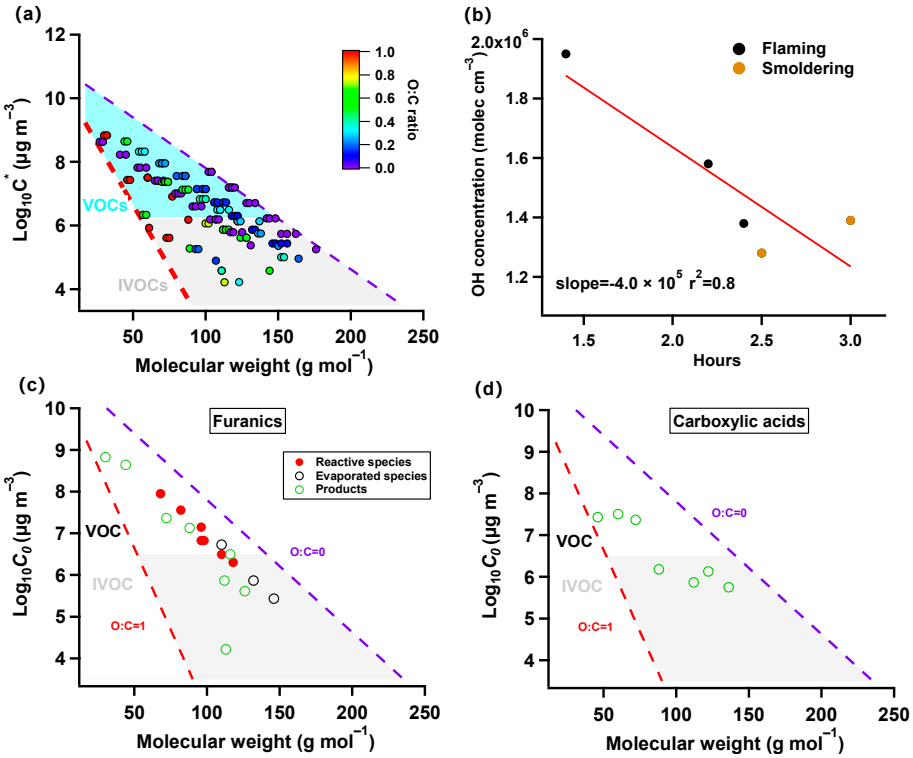



**Figure 4.** Saturation mass concentration ($C_0$) vs. molecular corridors of molar mass (M) vs. all NMOCs detected in elemental composition (**a**); estimated OH radical concentration (**b**); $C_0$ vs. M for furans and carboxylic acids (**c**,**d**).

Carboxylic acid compounds showed significant increases during photochemical aging. In the flaming and smoldering aging experiments, the carboxylic acid compound concentrations approximately doubled after the reaction (Figure 3). These carboxylic acids are gas-phase oxidation products, and their concentrations increased throughout the experiment compared to the initial emissions, encompassing both the smaller, more volatile VOCs and the less volatile IVOCs (Figure 4d). It has also been found in previous studies that

carboxylic acids can be gradually generated as oxidation products of aromatic hydrocarbons, phenols, and furans during the chemical aging process [36,54]. Furthermore, SOA degradation occurring in the atmosphere can also generate gaseous organic carboxylic acids [57].

### *3.4. Implications for Residential Biomass Burning SOA*

The results shown above indicate that the plume emitted from flaming and smoldering residential biomass combustion contains significant SOA precursors, not only including traditional compounds, such as benzene and carbonyl compounds, but also phenols and furans. These non-traditional compounds contribute significantly to SOA formation and exhibit strong reactivity (with a lifetime of less than 1 day under standard atmospheric conditions) and should be considered efficient SOA precursors. However, they are not fully accounted for in traditional SOA models. In the literature, SOA yields have only been clearly documented for a small fraction of numerous NMOCs in the atmosphere. Additionally, there are other compounds that contribute to SOA formation, but their yields are uncertain. A subset of these compounds is considered IVOCs, which fall into two main categories: one consists of compounds with determined structures, with each molecule containing at least six carbon atoms (explicitly listed in Table S3); the other consists of compounds with undetermined structures, but each molecule is expected to contain at least six carbon atoms. For these two categories of compounds, the SOA yields are estimated based on existing data and average values provided in the latest literature.

We estimated the contribution of residential biomass burning-sourced NMOCs to the SOA formation potential during photo-oxidation. The total SOA formed by organic compounds was estimated by multiplying the EF of the organic compounds by the SOA yield utilized in Table S3. The net OA mass enhancement ratio, denoted as the SOA generation rate (aged/fresh OA), is characterized by the ratio of OA mass following the aging process to the initial OA mass prior to aging. It is imperative to note that the accurate estimation of the OA enhancement ratio necessitates a careful consideration of wall-deposited particles. Figure 5 presents the functional relationship between the OA enhancement ratio obtained from the measured values and the calculated values based on the updated NMOC SOA yields (Table S3). The results indicate that by taking into account non-traditional SOA precursors and IVOC yields, the simulated values can better represent the actual SOA formation. Under atmospheric aging conditions, relatively low concentrations of NMOGs can lead to the majority of SOA being produced by residential biomass combustion. This finding, along with the identification of these key NMOGs, has implications for current conventional environmental measurement methods and SOA model parameterization.

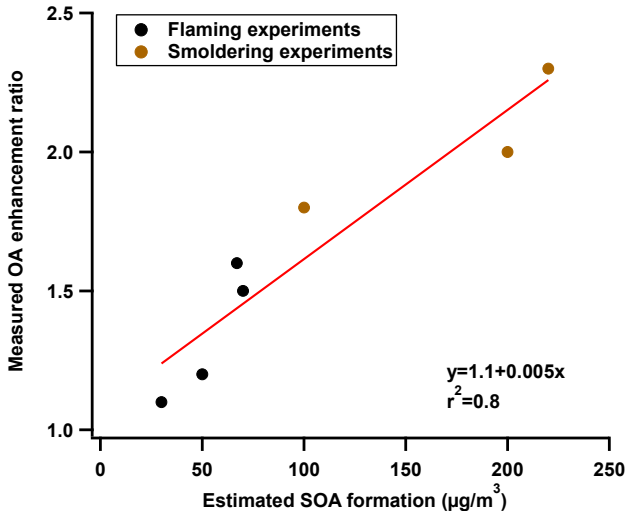



**Figure 5.** The functional relationship between the OA enhancement ratio obtained from measured values and the calculated values based on the updated NMOC SOA yields.

## 4. Conclusions

This study focused on commonly used biomass fuel and established a combustion laboratory to simulate residential biomass burning. The emission characteristics of NMOCs from residential biomass combustion were investigated, highlighting significant differences between the flaming and smoldering stages of combustion. The smoldering phase emitted significantly higher levels of NMOCs, which were approximately two to four times higher than those in the flaming phase. Additionally, the photochemical aging processes of VOCs and IVOCs were analyzed in detail using a chamber aging system. Furans, phenols, and some IVOCs were identified as important non-traditional precursors of SOA, with more than half of them being consumed during short atmospheric aging. Considering the yields of these non-traditional SOA precursors and IVOCs in SOA prediction models can help minimize discrepancies between simulated and measured SOA.

This study's results emphasize the necessity of routinely monitoring NMOGs that can produce SOA from residential biomass combustion. In the absence of routine monitoring for phenols, furans, and a range of IVOCs, there may be significant gaps in emission inventories, especially considering the inherent uncertainty in residential biomass combustion. In future emission studies, measuring these NMOGs is crucial to determine whether these compounds can explain the emissions produced under different combustion conditions and the formation of SOA from other sources. By reducing emissions of the key NMOGs that contribute the most to SOA formation, the SOA generated from residential wood combustion can be significantly reduced. Future research should also further consider more complex atmospheric aging environments to accurately assess and predict SOA formation from biomass combustion emissions.

**Supplementary Materials:** The following supporting information can be downloaded at: https://www.mdpi.com/article/10.3390/atmos15060692/s1, Table S1: Experimental details for aging experiments; Table S2: Summary of NMOCs species measured by the PTR-ToF-MS, for ion m/z and compounds. the saturation concentration (log C∗) of each compound was estimated using the parameterization, which is based solely on molecular formulas and thus can be readily applied to both identified and unidentified compounds at 298 K; Table S3: SOA yield used in this study.

**Author Contributions:** Conceptualization, S.L.; methodology, R.L.; software, K.H.; validation, R.L., Y.W. and X.J.; formal analysis, S.L., R.L. and X.J.; investigation, R.L., and S.L.; data curation, R.L., S.L. and K.H.; writing—original draft preparation, R.L. and S.L.; writing—review and editing, S.L. and R.L.; visualization, R.L. and S.L.; supervision, S.L. and X.J.; funding acquisition, R.L., S.L., Y.W., and K.H. All authors have read and agreed to the published version of the manuscript.

**Funding:** This research was funded by the National Natural Science Foundation of China (Grant 42175116); China Postdoctoral Science Foundation (2023M741773); Scientific Research Foundation for Guilin University of Technology (GUTQDJJ2023046).

**Institutional Review Board Statement:** Not applicable.

**Informed Consent Statement:** Not applicable.

**Data Availability Statement:** The data presented in this study are available on request from the corresponding author. The data are not publicly available due to privacy.

**Acknowledgments:** We acknowledge the financial, technical, and personnel support provided by Beijing Aolongston Technology Development Co., LTD.

**Conflicts of Interest:** The authors declare no conflicts of interest.

## References

1. Jathar, S.H.; Gordon, T.D.; Hennigan, C.J.; Pye, H.O.; Pouliot, G.; Adams, P.J.; Donahue, N.M.; Robinson, A.L. Unspeciated organic emissions from combustion sources and their influence on the secondary organic aerosol budget in the United States. *Proc. Natl. Acad. Sci. USA* **2014**, *111*, 10473–10478. [CrossRef] [PubMed]
2. Butt, E.W.; Rap, A.; Schmidt, A.; Scott, C.E.; Pringle, K.J.; Reddington, C.L.; Richards, N.A.D.; Woodhouse, M.T.; Ramirez-Villegas, J.; Yang, H.; et al. The impact of residential combustion emissions on atmospheric aerosol, human health, and climate. *Atmos. Chem. Phys.* **2016**, *16*, 873–905. [CrossRef]

3. Wu, W.; Zhao, B.; Wang, S.; Hao, J. Ozone and secondary organic aerosol formation potential from anthropogenic volatile organic compounds emissions in China. *J. Environ. Sci.* **2017**, *53*, 224–237. [CrossRef] [PubMed]
4. Robinson, A.L.; Donahue, N.M.; Shrivastava, M.K.; Weitkamp, E.A.; Sage, A.M.; Grieshop, A.P.; Lane, T.E.; Pierce, J.R.; Pandis, S.N. Rethinking organic aerosols: Semivolatile emissions and photochemical aging. *Science* **2007**, *315*, 1259–1262. [CrossRef]
5. Cai, S.; Wang, Y.; Zhao, B.; Wang, S.; Chang, X.; Hao, J. The impact of the "Air Pollution Prevention and Control Action Plan" on $PM_{2.5}$ concentrations in Jing-Jin-Ji region during 2012–2020. *Sci. Total. Environ.* **2017**, *580*, 197–209. [CrossRef] [PubMed]
6. Mitchell, E.J.S.; Lea-Langton, A.R.; Jones, J.M.; Williams, A.; Layden, P.; Johnson, R. The impact of fuel properties on the emissions from the combustion of biomass and other solid fuels in a fixed bed domestic stove. *Fuel Process Technol.* **2016**, *142*, 115–123. [CrossRef]
7. Elsasser, M.; Busch, C.; Orasche, J.; Schön, C.; Hartmann, H.; Schnelle-Kreis, J.; Zimmermann, R. Dynamic Changes of the Aerosol Composition and Concentration during Different Burning Phases of Wood Combustion. *Energy Fuel* **2013**, *27*, 4959–4968. [CrossRef]
8. Goldstein, A.H.; Galbally, I.E. Known and unexplored organic constituents in the earth's atmosphere. *Environ. Sci. Technol.* **2007**, *41*, 1514–1521. [CrossRef] [PubMed]
9. Shiraiwa, M.; Berkemeier, T.; Schilling-Fahnestock, K.A.; Seinfeld, J.H.; Pöschl, U. Molecular corridors and kinetic regimes in the multiphase chemical evolution of secondary organic aerosol. *Atmos. Chem. Phys.* **2014**, *14*, 8323–8341. [CrossRef]
10. Donahue, N.M.; Robinson, A.L.; Stanier, C.O.; Pandis, S.N. Coupled partitioning, dilution, and dhemical aging of semivolatile organics. *Environ. Sci. Technol.* **2006**, *40*, 2635–2643. [CrossRef]
11. Kroll, J.H.; Smith, J.D.; Che, D.L.; Kessler, S.H.; Worsnop, D.R.; Wilson, K.R. Measurement of fragmentation and functionalization pathways in the heterogeneous oxidation of oxidized organic aerosol. *Phys. Chem. Chem. Phys.* **2009**, *11*, 8005–8014. [CrossRef] [PubMed]
12. Jathar, S.; Cappa, C.; Wexler, A.; Seinfeld, J.; Kleeman, M.J. Multi-generational oxidation model to simulate secondary organic aerosol in a 3-D air quality model. *Geosci. Model. Dev.* **2015**, *8*, 1857–1891. [CrossRef]
13. He, K.; Fu, T.; Zhang, B.; Xu, H.; Sun, J.; Zou, H.; Zhang, Z.; Hang Ho, S.S.; Cao, J.; Shen, Z. Examination of long-time aging process on volatile organic compounds emitted from solid fuel combustion in a rural area of China. *Chemosphere* **2023**, *333*, 138957. [CrossRef] [PubMed]
14. Natarajan, S.; Mukhopadhyay, K.; Thangaswamy, D.; Natarajan, A.; Chakraborty, D. Characterisation of indoor volatile organic compounds and its association with respiratory symptoms among children living in solid fuel using households in Tamil Nadu, India. *Mapan* **2022**, *37*, 565–578. [CrossRef]
15. Zhang, Y.; Kong, S.; Sheng, J.; Zhao, D.; Ding, D.; Yao, L.; Zheng, H.; Wu, J.; Cheng, Y.; Yan, Q.; et al. Real-time emission and stage-dependent emission factors/ratios of specific volatile organic compounds from residential biomass combustion in China. *Atmos. Res.* **2021**, *248*, 105189. [CrossRef]
16. Vakkari, V.; Kerminen, V.-M.; Beukes, J.P.; Tiitta, P.; van Zyl, P.G.; Josipovic, M.; Venter, A.D.; Jaars, K.; Worsnop, D.R.; Kulmala, M.; et al. Rapid changes in biomass burning aerosols by atmospheric oxidation. *Geophys. Res. Lett.* **2014**, *41*, 2644–2651. [CrossRef]
17. Ortega, A.M.; Day, D.A.; Cubison, M.J.; Brune, W.H.; Bon, D.; de Gouw, J.A.; Jimenez, J.L. Secondary organic aerosol formation and primary organic aerosol oxidation from biomass-burning smoke in a flow reactor during FLAME-3. *Atmos. Chem. Phys.* **2013**, *13*, 11551–11571. [CrossRef]
18. Shrivastava, M.; Cappa, C.D.; Fan, J.; Goldstein, A.H.; Guenther, A.B.; Jimenez, J.L.; Kuang, C.; Laskin, A.; Martin, S.T.; Ng, N.L.; et al. Recent advances in understanding secondary organic aerosol: Implications for global climate forcing. *Rev. Geophys.* **2017**, *55*, 509–559. [CrossRef]
19. Niu, X.; Li, J.; Wang, Q.; Ho, S.S.H.; Sun, J.; Li, L.; Cao, J.; Ho, K.F. Characteristics of fresh and aged volatile organic compounds from open burning of crop residues. *Sci. Total. Environ.* **2020**, *726*, 138545. [CrossRef]
20. Romanias, M.N.; Coggon, M.M.; Al Ali, F.; Burkholder, J.B.; Dagaut, P.; Decker, Z.; Warneke, C.; Stockwell, C.E.; Roberts, J.M.; Tomas, A.; et al. Emissions and atmospheric chemistry of furanoids from biomass burning: Insights from laboratory to atmospheric observations. *ACS Earth Space Chem.* **2024**, *8*, 857–899. [CrossRef]
21. Gilman, J.B.; Lerner, B.M.; Kuster, W.C.; Goldan, P.D.; Warneke, C.; Veres, P.R.; Roberts, J.M.; de Gouw, J.A.; Burling, I.R.; Yokelson, R.J. Biomass burning emissions and potential air quality impacts of volatile organic compounds and other trace gases from fuels common in the US. *Atmos. Chem. Phys.* **2015**, *15*, 13915–13938. [CrossRef]
22. Hatch, L.E.; Luo, W.; Pankow, J.F.; Yokelson, R.J.; Stockwell, C.E.; Barsanti, K.C. Identification and quantification of gaseous organic compounds emitted from biomass burning using two-dimensional gas chromatography–time-of-flight mass spectrometry. *Atmos. Chem. Phys.* **2015**, *15*, 1865–1899. [CrossRef]
23. Bhattu, D.; Zotter, P.; Zhou, J.; Stefenelli, G.; Klein, F.; Bertrand, A.; Temime-Roussel, B.; Marchand, N.; Slowik, J.G.; Baltensperger, U.; et al. Effect of stove technology and combustion conditions on gas and particulate emissions from residential biomass combustion. *Environ. Sci. Technol.* **2019**, *53*, 2209–2219. [CrossRef] [PubMed]
24. Bruns, E.A.; Slowik, J.G.; El Haddad, I.; Kilic, D.; Klein, F.; Dommen, J.; Temime-Roussel, B.; Marchand, N.; Baltensperger, U.; Prévôt, A.S.H. Characterization of gas-phase organics using proton transfer reaction time-of-flight mass spectrometry: Fresh and aged residential wood combustion emissions. *Atmos. Chem. Phys.* **2017**, *17*, 705–720. [CrossRef]

25. Desservettaz, M.; Pikridas, M.; Stavroulas, I.; Bougiatioti, A.; Liakakou, E.; Hatzianastassiou, N.; Sciare, J.; Mihalopoulos, N.; Bourtsoukidis, E. Emission of volatile organic compounds from residential biomass burning and their rapid chemical transformations. *Sci. Total. Environ.* **2023**, *903*, 166592. [CrossRef] [PubMed]
26. Stockwell, C.E.; Veres, P.R.; Williams, J.; Yokelson, R.J. Characterization of biomass burning emissions from cooking fires, peat, crop residue, and other fuels with high-resolution proton-transfer-reaction time-of-flight mass spectrometry. *Atmos. Chem. Phys.* **2015**, *15*, 845–865. [CrossRef]
27. Yokelson, R.J.; Burling, I.R.; Gilman, J.B.; Warneke, C.; Stockwell, C.E.; de Gouw, J.; Akagi, S.K.; Urbanski, S.P.; Veres, P.; Roberts, J.M.; et al. Coupling field and laboratory measurements to estimate the emission factors of identified and unidentified trace gases for prescribed fires. *Atmos. Chem. Phys.* **2013**, *13*, 89–116. [CrossRef]
28. Donahue, N.M.; Robinson, A.L.; Pandis, S.N. Atmospheric organic particulate matter: From smoke to secondary organic aerosol. *Atmos. Environ.* **2009**, *43*, 94–106. [CrossRef]
29. Jimenez, J.L.; Canagaratna, M.; Donahue, N.; Prevot, A.; Zhang, Q.; Kroll, J.H.; DeCarlo, P.F.; Allan, J.D.; Coe, H.; Ng, N.J.; et al. Evolution of organic aerosols in the atmosphere. *Science* **2009**, *326*, 1525–1529. [CrossRef]
30. Li, S.; Liu, D.; Wu, Y.; Hu, K.; Jiang, X.; Tian, P.; Sheng, J.; Pan, B.; Zhao, D. Aging effects on residential biomass burning emissions under quasi-real atmospheric conditions. *Environ. Pollut.* **2023**, *337*, 122615. [CrossRef]
31. Li, S.; Liu, D.; Hu, D.; Kong, S.; Wu, Y.; Ding, S.; Cheng, Y.; Qiu, H.; Zheng, S.; Yan, Q.; et al. Evolution of organic aerosol from wood smoke influenced by burning phase and solar radiation. *J. Geophys. Res.-Atmos.* **2021**, *126*, e2021JD034534. [CrossRef]
32. Lindinger, W.; Hansel, A.; Jordan, A. On-line monitoring of volatile organic compounds at pptv levels by means of proton-transfer-reaction mass spectrometry (PTR-MS) medical applications, food control and environmental research. *Int. J. Mass Spectrom. Ion Process.* **1998**, *173*, 191–241. [CrossRef]
33. Wu, Y.; Liu, D.; Tian, P.; Sheng, J.; Liu, Q.; Li, R.; Hu, K.; Jiang, X.; Li, S.; Bi, K.; et al. Tracing the formation of secondary aerosols influenced by solar radiation and relative humidity in suburban environment. *J. Geophys. Res.-Atmos.* **2022**, *127*, e2022JD036913. [CrossRef]
34. Bruns, E.A.; El Haddad, I.; Slowik, J.G.; Kilic, D.; Klein, F.; Baltensperger, U.; Prévôt, A.S.H. Identification of significant precursor gases of secondary organic aerosols from residential wood combustion. *Sci. Rep.* **2016**, *6*, 27881. [CrossRef] [PubMed]
35. Hartikainen, A.; Yli-Pirilä, P.; Tiitta, P.; Leskinen, A.; Kortelainen, M.; Orasche, J.; Schnelle-Kreis, J.; Lehtinen, K.E.J.; Zimmermann, R.; Jokiniemi, J.; et al. Volatile organic compounds from logwood combustion: Emissions and transformation under dark and photochemical aging conditions in a smog chamber. *Environ. Sci. Technol.* **2018**, *52*, 4979–4988. [CrossRef] [PubMed]
36. Yee, L.D.; Kautzman, K.E.; Loza, C.L.; Schilling, K.A.; Coggon, M.M.; Chhabra, P.S.; Chan, M.N.; Chan, A.W.H.; Hersey, S.P.; Crounse, J.D.; et al. Secondary organic aerosol formation from biomass burning intermediates: Phenol and methoxyphenols. *Atmos. Chem. Phys.* **2013**, *13*, 8019–8043. [CrossRef]
37. Fang, Z.; Deng, W.; Zhang, Y.; Ding, X.; Tang, M.; Liu, T.; Hu, Q.; Zhu, M.; Wang, Z.; Yang, W.; et al. Open burning of rice, corn and wheat straws: Primary emissions, photochemical aging, and secondary organic aerosol formation. *Atmos. Chem. Phys.* **2017**, *17*, 14821–14839. [CrossRef]
38. Chan, A.W.H.; Kautzman, K.E.; Chhabra, P.S.; Surratt, J.D.; Chan, M.N.; Crounse, J.D.; Kürten, A.; Wennberg, P.O.; Flagan, R.C.; Seinfeld, J.H. Secondary organic aerosol formation from photooxidation of naphthalene and alkylnaphthalenes: Implications for oxidation of intermediate volatility organic compounds (IVOCs). *Atmos. Chem. Phys.* **2009**, *9*, 3049–3060. [CrossRef]
39. Donahue, N.M.; Epstein, S.A.; Pandis, S.N.; Robinson, A.L. A two-dimensional volatility basis set: 1. organic-aerosol mixing thermodynamics. *Atmos. Chem. Phys.* **2011**, *11*, 3303–3318. [CrossRef]
40. Li, Y.; Pöschl, U.; Shiraiwa, M. Molecular corridors and parameterizations of volatility in the chemical evolution of organic aerosols. *Atmos. Chem. Phys.* **2016**, *16*, 3327–3344. [CrossRef]
41. Akagi, S.K.; Yokelson, R.J.; Wiedinmyer, C.; Alvarado, M.J.; Reid, J.S.; Karl, T.; Crounse, J.D.; Wennberg, P.O. Emission factors for open and domestic biomass burning for use in atmospheric models. *Atmos. Chem. Phys.* **2011**, *11*, 4039–4072. [CrossRef]
42. Sinha, P.; Hobbs, P.V.; Yokelson, R.J.; Bertschi, I.T.; Blake, D.R.; Simpson, I.J.; Gao, S.; Kirchstetter, T.W.; Novakov, T. Emissions of trace gases and particles from savanna fires in southern Africa. *J. Geophys. Res.-Atmos.* **2003**, *108*. [CrossRef]
43. Stefenelli, G.; Jiang, J.; Bertrand, A.; Bruns, E.A.; Pieber, S.M.; Baltensperger, U.; Marchand, N.; Aksoyoglu, S.; Prévôt, A.S.H.; Slowik, J.G.; et al. Secondary organic aerosol formation from smoldering and flaming combustion of biomass: A box model parametrization based on volatility basis set. *Atmos. Chem. Phys.* **2019**, *19*, 11461–11484. [CrossRef]
44. Parandaman, A.; Kumar, M.; Francisco, J.S.; Sinha, A. Organic acid formation from the atmospheric oxidation of gem diols: Reaction mechanism, energetics, and rates. *J. Phys. Chem. A* **2018**, *122*, 6266–6276. [CrossRef] [PubMed]
45. Fu, T.-M.; Jacob, D.J.; Wittrock, F.; Burrows, J.P.; Vrekoussis, M.; Henze, D.K. Global budgets of atmospheric glyoxal and methylglyoxal, and implications for formation of secondary organic aerosols. *J. Geophys. Res.-Atmos.* **2008**, *113*. [CrossRef]
46. Kawamura, K.; Okuzawa, K.; Aggarwal, S.G.; Irie, H.; Kanaya, Y.; Wang, Z. Determination of gaseous and particulate carbonyls (glycolaldehyde, hydroxyacetone, glyoxal, methylglyoxal, nonanal and decanal) in the atmosphere at Mt. Tai. *Atmos. Chem. Phys.* **2013**, *13*, 5369–5380. [CrossRef]
47. Andreae, M.O.; Merlet, P. Emission of trace gases and aerosols from biomass burning. *Glob. Biogeochem. Cycles* **2001**, *15*, 955–966. [CrossRef]
48. Henze, D.K.; Seinfeld, J.H.; Ng, N.L.; Kroll, J.H.; Fu, T.M.; Jacob, D.J.; Heald, C.L. Global modeling of secondary organic aerosol formation from aromatic hydrocarbons: High- vs. low-yield pathways. *Atmos. Chem. Phys.* **2008**, *8*, 2405–2420. [CrossRef]

49. Phousongphouang, P.T.; Arey, J. Rate constants for the gas-phase reactions of a series of alkylnaphthalenes with the OH radical. *Environ. Sci. Technol.* **2002**, *36*, 1947–1952. [CrossRef]
50. Ziemann, P.J.; Atkinson, R. Kinetics, products, and mechanisms of secondary organic aerosol formation. *Chem. Soc. Rev.* **2012**, *41*, 6582–6605. [CrossRef]
51. Ng, N.L.; Kroll, J.H.; Chan, A.W.H.; Chhabra, P.S.; Flagan, R.C.; Seinfeld, J.H. Secondary organic aerosol formation from m-xylene, toluene, and benzene. *Atmos. Chem. Phys.* **2007**, *7*, 3909–3922. [CrossRef]
52. Xiao, Y.; Hu, M.; Li, X.; Zong, T.; Xu, N.; Hu, S.; Zeng, L.; Chen, S.; Song, Y.; Guo, S.; et al. Aqueous secondary organic aerosol formation attributed to phenols from biomass burning. *Sci. Total. Environ.* **2022**, *847*, 157582. [CrossRef] [PubMed]
53. Hatch, L.E.; Yokelson, R.J.; Stockwell, C.E.; Veres, P.R.; Simpson, I.J.; Blake, D.R.; Orlando, J.J.; Barsanti, K.C. Multi-instrument comparison and compilation of non-methane organic gas emissions from biomass burning and implications for smoke-derived secondary organic aerosol precursors. *Atmos. Chem. Phys.* **2017**, *17*, 1471–1489. [CrossRef]
54. Coggon, M.M.; Lim, C.Y.; Koss, A.R.; Sekimoto, K.; Yuan, B.; Gilman, J.B.; Hagan, D.H.; Selimovic, V.; Zarzana, K.J.; Brown, S.S.; et al. OH chemistry of non-methane organic gases (NMOGs) emitted from laboratory and ambient biomass burning smoke: Evaluating the influence of furans and oxygenated aromatics on ozone and secondary NMOG formation. *Atmos. Chem. Phys.* **2019**, *19*, 14875–14899. [CrossRef]
55. Arathala, P.; Tangtartharakul, C.B.; Sinha, A. Atmospheric ring-closure and dehydration reactions of 1,4-hydroxycarbonyls in the gas phase: The impact of catalysts. *J. Phys. Chem. A* **2021**, *125*, 5963–5975. [CrossRef] [PubMed]
56. Koss, A.R.; Sekimoto, K.; Gilman, J.B.; Selimovic, V.; Coggon, M.M.; Zarzana, K.J.; Yuan, B.; Lerner, B.M.; Brown, S.S.; Jimenez, J.L.; et al. Non-methane organic gas emissions from biomass burning: Identification, quantification, and emission factors from PTR-ToF during the FIREX 2016 laboratory experiment. *Atmos. Chem. Phys.* **2018**, *18*, 3299–3319. [CrossRef]
57. Li, Y.J.; Huang, D.D.; Cheung, H.Y.; Lee, A.K.Y.; Chan, C.K. Aqueous-phase photochemical oxidation and direct photolysis of vanillin—A model compound of methoxy phenols from biomass burning. *Atmos. Chem. Phys.* **2014**, *14*, 2871–2885. [CrossRef]


**Disclaimer/Publisher's Note:** The statements, opinions and data contained in all publications are solely those of the individual author(s) and contributor(s) and not of MDPI and/or the editor(s). MDPI and/or the editor(s) disclaim responsibility for any injury to people or property resulting from any ideas, methods, instructions or products referred to in the content.